ChemPubSoc Europe

DOI: 10.1002/chem.201503040

CHEMISTRY A European Journal Full Paper

Fluorescent Dyes | *Hot Paper*

Tailoring the Solid-State Fluorescence Emission of BODIPY Dyes by *meso* Substitution**

Sungwoo Kim,[a] Jean Bouffard,*[b] and Youngmi Kim*[a]

Abstract: 4,4-Difluoro-4-bora-3a,4a-diaza-*s*-indacene (BODIPY) derivatives bearing varied substituents at the *meso* position (i.e., CF_3, CH_3, COOR, CHO, CN, Cl, *i*Pr) were synthesized to elucidate the structure–property relationships that give rise to emissive J-aggregates. Several new BODIPY derivatives can be added to the previously reported 1,3,5,7-tetramethyl-8-trifluoromethyl derivative to the list of those forming J-aggregates, in addition to other dyes that are emissive in the solid state without forming J-aggregates.

Introduction

4,4-Difluoro-4-bora-3a,4a-diaza-*s*-indacene (BODIPY) dyes are ubiquitous in multiple areas of materials science thanks to their high chemical and photochemical stabilities, relatively large molar absorption coefficients, narrow emission bands and high fluorescence quantum yields.[1] The figures of merit are, however, mostly limited to dilute solutions, owing to the tendency of these largely planar aromatic dyes to form non-emissive aggregates in condensed states.[2] The introduction of highly sterically demanding substituents on the periphery of the BODIPY has been shown to block the formation of aggregates to some extent, but this approach typically has the shortcoming of requiring elaborate multistep syntheses.[3]

An alternative approach consists in the engineering dyes that favor the formation of emissive aggregates.[4] The so-called aggregation-induced emission (or aggregation-induced enhanced emission)—AIE(E)—approach has so far been shown to be successful for a small number of BODIPY dyes, especially when the increase in rigidity that accompanies aggregation can suppress nonradiative deactivation pathways.[5] In 2014, we reported that the introduction of a CF_3 group at the *meso* position (C8) of a BODIPY dye (CF_3-**T1**, Scheme 1) resulted in a striking AIE feature that stood in sharp contrast with the typical condensed-phase emission quenching of BODIPY dyes such as *meso*-CH_3-BODIPY, CH_3-**T2**.[6] It was also established, for the first time among BODIPY dyes, that this AIE feature originated from a different mechanism, the formation of a J-type excitonic coupling between adjacent dye molecules in the crystal and in the aggregates.[7]

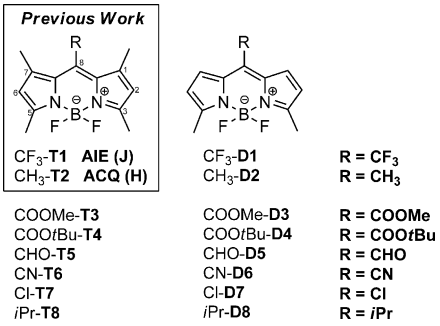

Scheme 1. Structures of *meso*-substituted BODIPY dyes.

In this paper, we present a systematic study of the substituents at the periphery of BODIPY dyes, in particular the *meso* substituents, to elucidate the factors that govern the formation of emissive J-aggregates in this family of fluorophores. Importantly, it was found that, although unreported before 2014, the formation of emissive BODIPY J-aggregates is not limited to the trifluoromethyl-substituted CF_3-**T1**, but is in fact also found for several new derivatives. Finally, we demonstrate the potential of these J-aggregate-forming fluorophores for the solid-state sensing of chemical vapors.

Results and Discussion

Preparation of the BODIPY dyes

Sixteen members of the BODIPY family were prepared, consisting of eight pairs of *meso*-substituted 1,3,5,7-tetramethyl (**T**) and 3,5-dimethyl (**D**) derivatives (Scheme 1). These were subjected to spectroscopic and structural studies to elucidate the electronic and steric effects of substituents at the *meso* posi-

[a] *S. Kim, Prof. Y. Kim*
Department of Chemistry, Institute of Nanosensor and Biotechnology
Dankook University
152 Jukjeon-ro, Suji-gu, Yongin-si, Gyeonggi-do, 448-701 (Korea)
E-mail: youngmi@dankook.ac.kr

[b] *Prof. J. Bouffard*
Department of Chemistry and Nano Science (BK 21 Plus)
Ewha Womans University
52 Ewhayeodae-gil, Seodaemun-gu, Seoul 120-750 (Korea)
E-mail: bouffard@ewha.ac.kr

[**] *BODIPY = 4,4-difluoro-4-bora-3a,4a-diaza-s-indacene.*

Supporting information for this article is available on the WWW under http://dx.doi.org/10.1002/chem.201503040.

tion, and that of the flanking methyl groups at C1 and C7, on their structural and photophysical properties. The *meso*-substituted 1,3,5,7-tetramethyl and 3,5-dimethyl BODIPY dyes, CF_3-**T1** and -**D1**,[6] CH_3-**T2** and -**D2**,[6,8] COOMe-**T3** and -**D3**,[9] COO*t*Bu-**T4** and -**D4**,[9] CHO-**T5**[10] and -**D5**,[11] CN-**T6**[12] and Cl-**T7** and -**D7**[13] (Scheme 1), were prepared following slight modifications of previously described procedures. CN-**D6** was synthesized in two steps from CHO-**D5** by condensation with hydroxylamine to yield the corresponding oxime, which was then dehydrated with PPh_3 and *N*-chlorosuccinimide (NCS) (Scheme 2 A). *i*Pr-**D8** and *i*Pr-**T8** were synthesized by the reaction of the required pyrrole with *iso*-butyryl chloride in the presence of Et_3N followed by treatment with $BF_3{\cdot}OEt_2$ (Scheme 2 B). All the BODIPY derivatives are soluble in common organic solvents, such as THF, $CHCl_3$, acetone, and CH_3CN, but insoluble in water.

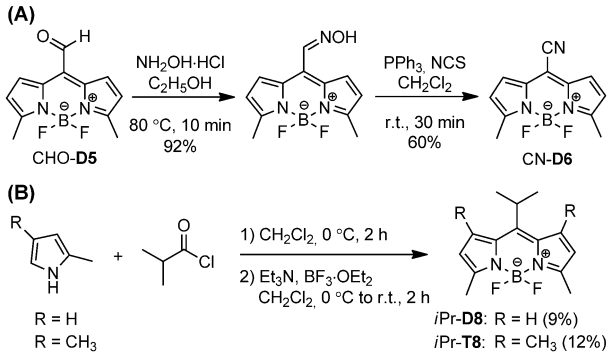

Scheme 2. Synthesis of *meso*-substituted BODIPYs CN-**D6** (A) and *i*Pr-**T8** and *i*Pr-**D8** (B).

Spectroscopic properties of the BODIPY dyes in solution

The absorption and fluorescence properties of the prepared 1,3,5,7-tetramethyl and 3,5-dimethyl BODIPYs in $CHCl_3$ solution are summarized in Table 1 and Figure 1. The absorption and emission profiles, and fluorescence quantum yields of the dyes in solution are greatly affected by *meso* substituents as well as methyl groups at C1 and C7. As previously observed for CF_3-**T1**,[6] introduction of electron-withdrawing *meso* substituents (i.e., CF_3-**D1**, COOMe-**3**, COO*t*Bu-**4**, CHO-**5**, CN-**6**) leads to bathochromic shifts with respect to analogues with alkyl substituents at the *meso* position (CH_3-**2** and *i*Pr-**8**). The absorption and emission maxima of *meso*-chloro-substituted BODIPYs (Cl-**7**) are, however, comparable to those of the corresponding *meso*-methyl-substituted BODIPYs (CH_3-**2**). As described earlier,[6] these observations are in qualitative agreement with DFT calculations, which indicate that electron-withdrawing substituents at the *meso* position preferentially stabilize the LUMO, resulting in a decreased HOMO–LUMO gap (see Figures S61–S64 in the Supporting Information).

Particularly interesting is the observation that 3,5-dimethyl BODIPYs substituted at the *meso* position with electron-withdrawing carbonyl groups (COOR and CHO) exhibit absorption and emission maxima that are redshifted more than those of their 1,3,5,7-tetramethyl counterparts. For example, the respective absorption ($\lambda_{abs.max}$) and emission ($\lambda_{em.max}$) maxima of COOMe-**D3** in $CHCl_3$ are at 541 nm and 604 nm, which is far to the red of COOMe-**T3** ($\lambda_{abs.max}=516$ nm, $\lambda_{em.max}=543$ nm). Similar trends exist in other 1,3,5,7-tetramethyl and 3,5-dimethyl BODIPYs (COO*t*Bu-**T4** vs. COO*t*Bu-**D4**; CHO-**T5** vs. CHO-**D5**). These differences are attributed to the flanking methyl groups at C1 and C7 in the 1,3,5,7-tetramethyl-BODIPY series (**T**), which force the electron-withdrawing groups at the *meso* position to pivot out of π-conjugation, reducing their electronic influence. Indeed, whereas the calculated optimized geometry for COOMe-**D3** shows an ester carbonyl conjugated with the BODIPY core (41° angle, Figure 2, right), that for COOMe-**T3** presents an ester carbonyl orthogonal to the boradiazaindacene plane (90° angle, Figure 2, left). In a similar fashion, the 3,5-dimethyl BODIPY analogues, COO*t*Bu-**D4** and CHO-**D5**, show much smaller torsion angles than their respective 1,3,5,7-tetramethyl counterparts, COO*t*Bu-**T4** and CHO-**T5** (Figures S62–63). Electronic conjugation is optimal for CHO-**D5**, which presents unusually redshifted absorption (600 nm) and emission (632 nm) bands, and for which calculations show a carbonyl group coplanar with the BODIPY plane. The opposite behavior is seen for CF_3-**D1** (544/563 nm) and CF_3-**T1** (553/622 nm). For dyes bearing this inductively electron-withdrawing but not π-conjugated group, preferential destabilization of

Table 1. Photophysical properties of the *meso*-substituted BODIPYs.[a]

Compound	λ_{abs} [nm]	ε ($\times10^4$) [$M^{-1}cm^{-1}$]	λ_{em} [nm]	Φ_F	τ_{av}[e] [ns]	k_r[f] [s^{-1}]	k_{nr}[g] [s^{-1}]	$\Delta\nu_{St}$ [cm^{-1}]	τ_{av}[e,h] [ns]
CF_3-**T1**	553	5.1	622	0.008[c]	0.21	3.8×10^7	4.7×10^9	2006	0.23
CF_3-**D1**	544	6.4	563	0.94[c]	6.51	1.4×10^8	9.2×10^6	620	7.06
CH_3-**T2**	499	11.6	520	1.00[b]	5.22	1.9×10^8	$\leq1.9\times10^6$	809	5.90
CH_3-**D2**	508	11.2	526	0.99[b]	5.30	1.9×10^8	1.9×10^6	674	6.12
COOMe-**T3**	516	10.3	543	0.005[b]	0.16	3.1×10^7	6.2×10^9	964	0.16
COOMe-**D3**	541	5.6	604	0.44[c]	7.26	6.1×10^7	7.7×10^7	1928	4.03
COO*t*Bu-**T4**	515	10.1	544	0.007[b]	0.19	3.7×10^7	5.2×10^9	1035	0.20
COO*t*Bu-**D4**	530	5.4	600	0.52[c]	7.34	7.1×10^7	6.5×10^7	2201	4.03
CHO-**T5**	515	5.7	545	0.002[b]	1.43	1.4×10^6	7.0×10^8	1069	2.15, 0.3[i]
CHO-**D5**	600	3.4	632	0.34[d]	4.81	7.1×10^7	1.4×10^8	844	n.a.[j]
CN-**T6**	561	7.1	585	0.50[c]	6.28	8.0×10^7	8.0×10^7	731	0.26
CN-**D6**	568	6.9	586	0.60[c]	7.24	1.0×10^8	6.8×10^7	541	6.46
Cl-**T7**	504	9.5	527	0.51[b]	3.99	1.3×10^8	1.2×10^8	866	0.24
Cl-**D7**	516	9.1	535	0.84[b]	5.54	1.5×10^8	2.9×10^7	688	6.38
*i*Pr-**T8**	508	9.0	545	0.014[b]	0.26	5.4×10^7	3.8×10^9	1336	0.63
*i*Pr-**D8**	509	8.4	528	0.90[b]	5.54	1.6×10^8	1.8×10^7	707	5.46

[a] In $CHCl_3$. [b] Quantum yields relative to fluorescein in 0.1 N NaOH ($\Phi_F=0.95$). [c] Quantum yields relative to rhodamine 6G in ethanol ($\Phi_F=0.95$). [d] Quantum yields relative to cresyl violet perchlorate in ethanol ($\Phi_F=0.54$). [e] The weighted mean lifetime. [f] $k_r=\Phi_F/\tau$. [g] $k_{nr}=(1-\Phi_F)/\tau$. [h] In 99:1 (v/v) water/CH_3CN. [i] $\tau_{av}=2.15$ ns for 540 nm and $\tau_{av}=0.3$ ns for 650 nm. [j] Not available due to its reactivity with water.[14]

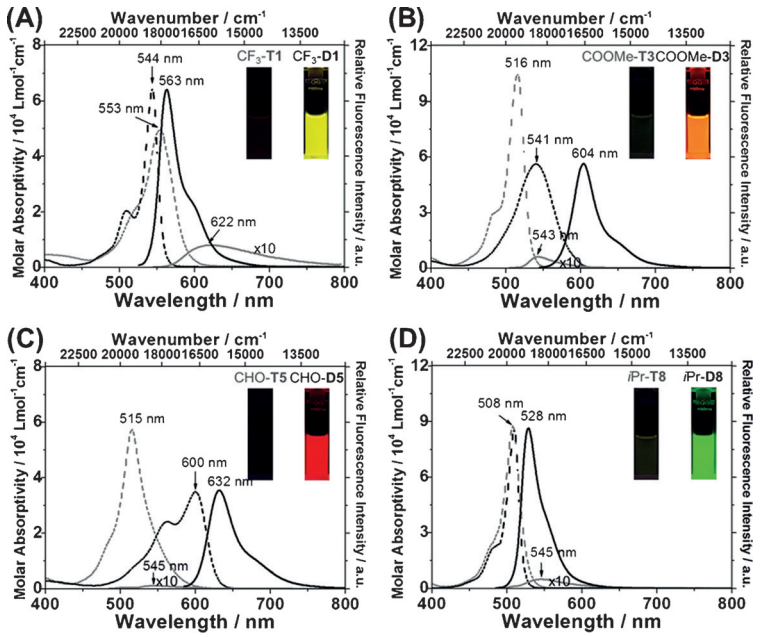

Figure 1. Absorption (dashed lines) and emission (solid lines) spectra of BODIPY dyes in $CHCl_3$ solutions (2×10^{-5} mol L^{-1}): (A) CF_3-**T1** (grey) and CF_3-**D1** (black); (B) COOMe-**T3** (grey) and COOMe-**D3** (black); (C) CHO-**T5** (grey) and CHO-**D5** (black); (D) *i*Pr-**T8** (grey) and *i*Pr-**D8** (black). Emission spectra of CF_3-**T1**, COOMe-**T3**, CHO-**T5**, and *i*Pr-**T8** are magnified 10-fold. Insets: photographs of each corresponding solution under irradiation at 365 nm.

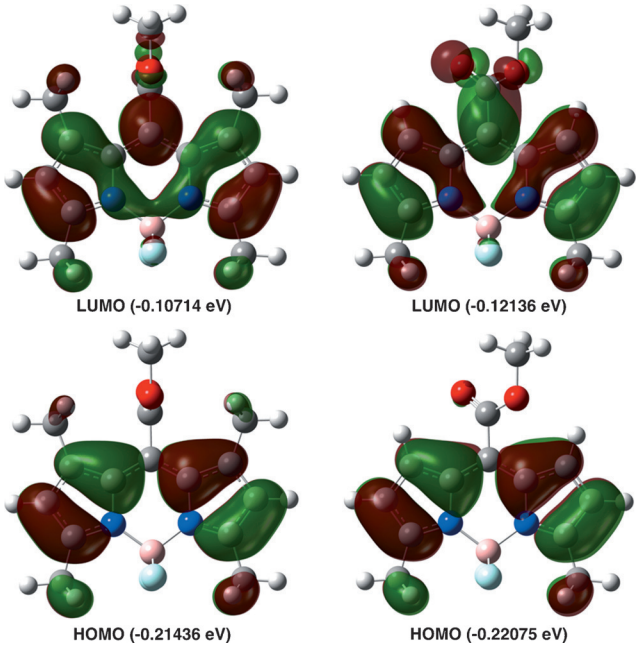

Figure 2. Calculated frontier molecular orbitals for COOMe-**T3** (left) and COOMe-**D3** (right) and their orbital energies.

the HOMO by the donating methyl groups results in a redshifted CF_3-**T1** (Figure S61).

Consequently, energies associated with the absorption maxima of 1,3,5,7-tetramethyl BODIPYs correlate well with the Hammett substituent constants, σ_p[15] (CN > CF_3 > COOMe > CHO > Cl > CH_3), for the *meso* groups. Conversely, the order of the transition energies of 3,5-dimethyl BODIPYs best correlate with the Hammett σ_{p-} values (CHO > CN > CF_3 > COOMe > Cl > CH_3) for the *meso* substituents.

The most striking difference that exists between the solution-phase photophysical properties of 1,3,5,7-tetramethyl and 3,5-dimethyl BODIPYs is seen in their fluorescence quantum yields (Φ_F). Specifically, regardless of the electronic properties of the *meso* substituents, nearly all 1,3,5,7-tetramethyl BODIPYs have lower Φ_F than those of their 3,5-dimethyl counterparts, ($\Phi_F = 0.008$ (CF_3-**T1**) vs. 0.94 (CF_3-**D1**); 0.005 (COOMe-**T3**) vs. 0.44 (COOMe-**D3**); 0.007 (COO*t*Bu-**T4**) vs. 0.52 (COO*t*Bu-**D4**); 0.002 (CHO-**T5**) vs. 0.34 (CHO-**D5**); 0.50 (CN-**T6**) vs. 0.60 (CN-**D6**); 0.51 (Cl-**T7**) vs. 0.84 (Cl-**D7**); 0.014 (*i*Pr-**T8**) vs. 0.90 (*i*Pr-**D8**)). Exceptions to this rule are CH_3-**T2** and CH_3-**D2**, which have similarly high Φ_F values of almost 1. Notably, 1,3,5,7-tetramethyl BODIPYs with electron-withdrawing *meso* groups (i.e., CF_3-**T1**, COOMe-**T3**, COO*t*Bu-**T4**, and CHO-**T5**) or a bulky electron-donating group (i.e., *i*Pr-**T8**) are non-emissive in solution ($\Phi_F < 0.015$), but their 3,5-dimethyl BODIPY counterparts have relatively high fluorescence quantum yields ranging from 0.34–0.94. Fluorescence lifetime analysis suggests that the depressed quantum yields for 1,3,5,7-tetramethyl BODIPYs reflect large rate constants for nonradiative deactivation (k_{nr}), which are approximately 10^2-fold larger than those for the 3,5-dimethyl BODIPY analogues (Table 1). Particularly sterically congested 1,3,5,7-tetramethyl BODIPYs show especially fast nonradiative deactivation ($k_{nr} > 1\times10^9$ s^{-1}), which is associated with deviations from planarity of the boradiazaindacene ring system in the ground state,[16] as confirmed by X-ray crystallography. For instance, the X-ray structures of *i*Pr-**T8** (Figure 3) and CF_3-**T1**[6] show significant deviations from planarity, reflected in the angle between the planes defined by the two pyrrole rings (*i*Pr-**T8**: 7.4°; CF_3-**T1**: 2.7°). In contrast, highly fluorescent CH_3-**T2** has a fully planar structure (0.0°).[6]

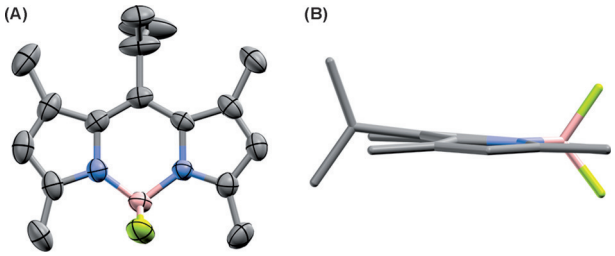

Figure 3. Top (A) and side (B) views of the molecular structure of *i*Pr-**T8**, with the thermal ellipsoids set at 50% probability. For clarity, the average position of the *i*Pr group (over equal occupancies) is shown and H atoms are omitted for clarity.

Evidence to support the proposal that the steric effects of *meso* substituents govern the rates of nonradiative decay of

1,3,5,7-tetramentyl BODIPYs was gained in studies exploring solvent viscosity effects. For this purpose, emission spectra of COOMe-**3** and *i*Pr-**8** were recorded in solutions containing varying composition of methanol and glycerol. The results show increases in fluorescence intensities of COOMe-**T3** (ca. 45-fold) and *i*Pr-**T8** (ca. 33-fold) as the fraction of the more viscous co-solvent (glycerol) increased from 9:1 to 1:9 methanol/glycerol (Figure 4A and C). In contrast, the fluorescence intensities of COOMe-**D3** and *i*Pr-**D8** do not significantly change as the viscosity of the medium increases (Figure 4B and D).

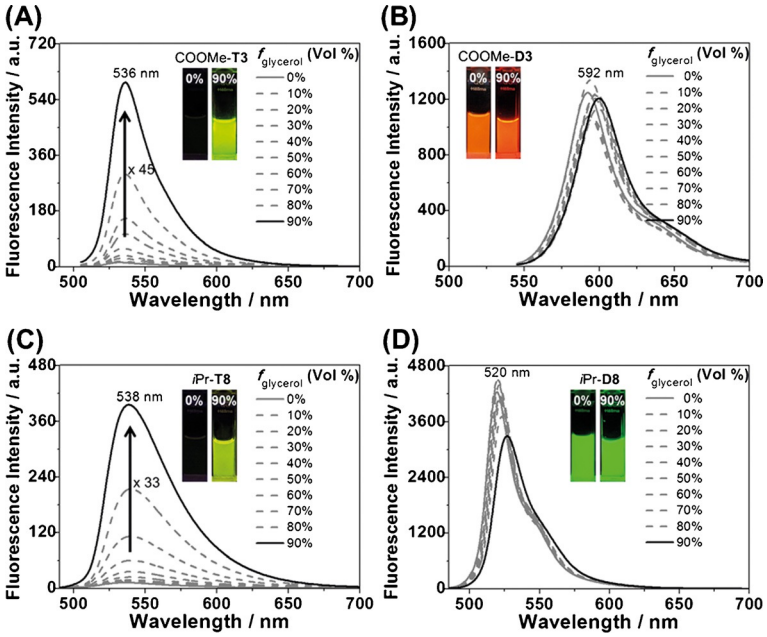

Figure 4. Emission spectra of COOMe-**T3** (A), COOMe-**D3** (B), *i*Pr-**T8** (C), and *i*Pr-**D8** (D) in glycerol-methanol mixtures with different glycerol fractions ($f_{glycerol}$). [COOMe-**T3**] = [COOMe-**D3**] = [*i*Pr-**T8**] = [*i*Pr-**D8**] = 20 μM. Excited at 490 nm (COOMe-**T3**), 530 nm (COOMe-**D3**), or 470 nm (*i*Pr-**T8** and *i*Pr-**D8**). Insets: photographs of each solution (in 0% (left) and 90% (right) glycerol in MeOH) under irradiation at 365 nm.

Spectroscopic properties of the BODIPY dyes in aggregates

The AIE behavior of the BODIPY dyes was investigated by promoting aggregate formation through alteration of solvent composition. The results show that a systematic change of composition of the CH_3CN/H_2O solvent system from 100% CH_3CN to 99% H_2O results in the formation of solid aggregates and is accompanied by marked changes in the absorption and emission spectra of the *meso*-substituted BODIPYs (Figures 5–7). In addition, *meso* substituents as well as their flanking methyl groups have pronounced effects on absorption and emission wavelengths and Φ_F of BODIPY dyes in the solid state.

Similar to CF_3-**T1**, which displays AIE features through J-aggregation,[6] 1,3,5,7-tetramethyl BODIPYs (COOMe-**T3** and COO*t*Bu-**T4**) with electron-withdrawing ester groups at *meso* positions become strong emitters and show the recognizable spectral changes associated with J-aggregate formation. As can be seen by inspection of the spectra displayed in Figure 5A, COOMe-**T3** has weak emission at 535 nm ($\Phi_F = 0.003$) in pure acetonitrile, but the emission intensity increases significantly when a large amount of water is present in the solvent ($f_w > 90\%$). Moreover, upon addition of water to a CH_3CN solution of COOMe-**T3**, a narrow redshifted absorption band ($\lambda_{abs.max} = 581$ nm) forms along with a narrow emission band with a small Stokes shift (176 cm^{-1}), and significantly enhanced efficiency (220-fold) is seen. Moreover, the fluorescence lifetime for COOMe-**T3** increases from 0.09 ns in CH_3CN solution to 0.16 ns in suspended aggregates. This change reflects a substantial increase in the fluorescence rate constant, $k_F = \Phi_F/\tau$, of COOMe-**T3** from 3.3×10^7 s^{-1} in solution to 4.4×10^8 s^{-1} in the aggregate state. Taken together, the changes in the photophysical properties of COOMe-**T3** are characteristic of J-aggregate formation, as previously reported for CF_3-**T1**.[6] A similar emission enhancement associated with the optical properties of J-aggregates is also observed for COO*t*Bu-**T4** (Figure 5B).

However, J-aggregation does not take place in the corresponding 3,5-dimethyl BODIPYs CF_3-**D1**, COOMe-**D3**, and COO*t*Bu-**D4** (Figures 6A–B and S22 in the Supporting Information). Instead, a typical aggregation-induced quenching response is observed, and fluorescence efficiencies decrease when the water content of CH_3CN solutions increases to 1:99 (v/v) CH_3CN/H_2O.

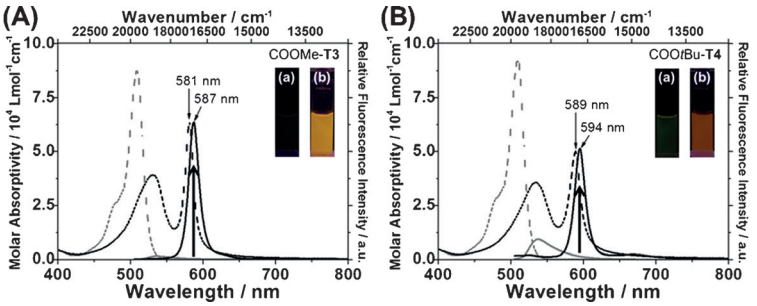

Figure 5. Absorption (dotted lines) and emission (solid lines) spectra of COOMe-**T3** (A) and COO*t*Bu-**T4** (B) at concentrations of 2×10^{-5} mol L^{-1} in CH_3CN (grey) and CH_3CN/H_2O solution (black, $CH_3CN/H_2O = 1:99$ (v/v)). Excitation at 490 nm. Insets: photographs of each solution (a: CH_3CN, b: $CH_3CN/H_2O = 1:99$ (v/v)) under irradiation at 365 nm.

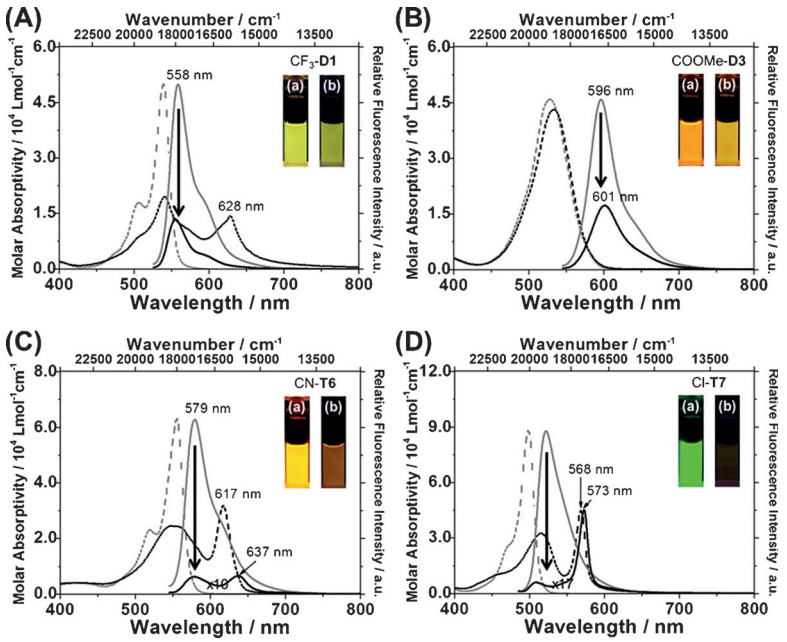

Figure 6. Absorption (dotted lines) and emission (solid lines) spectra of CF_3-**D1** (A), COOMe-**D3** (B), CN-**T6** (C), and Cl-**T7** (D) at concentrations of 2×10^{-5} mol L^{-1} in CH_3CN (grey) and CH_3CN/H_2O solution (black, $CH_3CN/H_2O = 1:99$ (v/v)). Excitation at 510 nm (CF_3-**D1**), 530 nm (COOMe-**D3** and CN-**T6**), or 470 nm (Cl-**T7**). Insets: photographs of each solution (a: CH_3CN, b: $CH_3CN/H_2O = 1:99$ (v/v)) under irradiation at 365 nm. Emission spectra of CN-**T6** and Cl-**T7** in $CH_3CN/H_2O = 1:99$ (v/v) are magnified 10-fold and 17-fold, respectively.

Studies were performed to elucidate the steric and electronic effects that lead to AIE behavior and the formation of J-aggregates of BODIPYs. For this purpose, the absorption and emission spectra of CN-**6**, Cl-**7**, and *i*Pr-**8** in CH_3CN/H_2O mixtures were recorded (Figures 6C–D, 7, and S24–S29). In the cases of CN-**T6** and Cl-**T7**, fluorescence emission intensity was found to decrease significantly upon aggregation (Figure 6C–D). This observation is ascribed to the strong tendency for π–π stacking of extended planar dyes (Figures S63–S64 in the Supporting Information). Indeed, both CN-**T6** and Cl-**T7** show the characteristic sharp and redshifted π-aggregation bands in their absorption spectra, but no emission bands comparable to those of COOMe-**T3** and COO*t*Bu-**T4**.

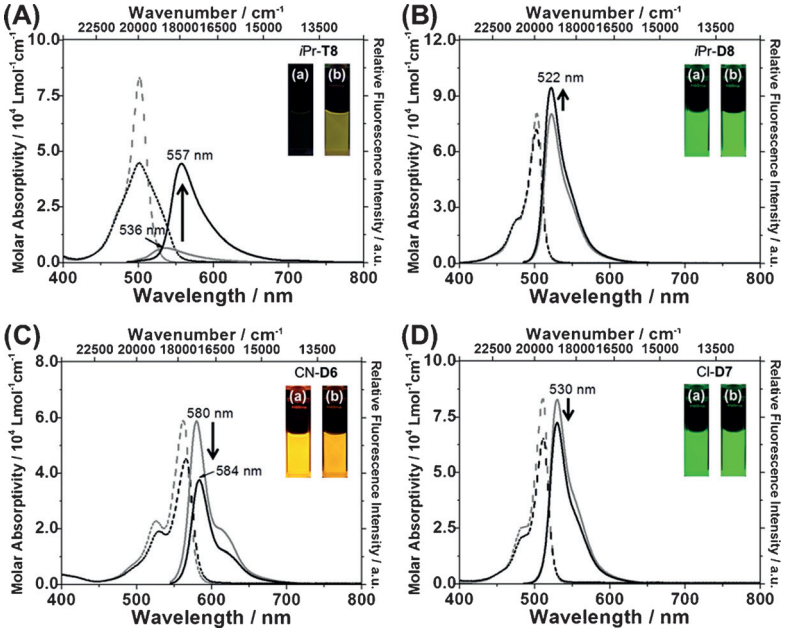

Figure 7. Absorption (dotted lines) and emission (solid lines) spectra of *i*Pr-**T8** (A), *i*Pr-**D8** (B), CN-**D6** (C), and Cl-**D7** (D) at concentrations of 2×10^{-5} mol L^{-1} in CH_3CN (grey) and CH_3CN/H_2O solution (black, $CH_3CN/H_2O = 1:99$ (v/v)). Excitation at 470 nm (*i*Pr-**T8**, *i*Pr-**D8**, and Cl-**D7**), or 530 nm (CN-**D6**). Insets: photographs of each solution (a: CH_3CN, b: $CH_3CN/H_2O = 1:99$ (v/v)) under irradiation at 365 nm.

The importance of sterically demanding substituents for the AIE behavior of BODIPYs is further reflected in the unusually enhanced emission intensity of *meso*-isopropyl-substituted 1,3,5,7-tetramethyl BODIPY (*i*Pr-**T8**) in aggregate suspensions containing large amounts of water ($f_w > 95\,\%$) (Figure 7A). However, spectroscopic features associated with J-aggregates (i.e., narrow redshifted absorption, nearly resonant fluorescence with narrow band, and increased fluorescence rate constant) were not observed for *i*Pr-**T8**. The fluorescence lifetime of *i*Pr-**T8**, which in CH_3CN is 0.28 ns, increases to 0.63 ns in 1:99 (v/v) CH_3CN/water mixtures, reflecting a slight decrease in k_F from 2.9×10^7 s^{-1} in solution to 2.5×10^7 s^{-1} in suspended aggregates. 3,5-Dimethyl BODIPYs substituted with *meso*-methyl (CH_3-**D2**, Figure S18 in the Supporting Information), methyl ester (COOMe-**D3**, Figure S20 in the Supporting Information), cyano (CN-**D6**, Figure 7C), chloro (Cl-**D7**, Figure 7D), and isopropyl (*i*Pr-**D8**, Figure 7B) groups are less prone to aggregation in CH_3CN solutions diluted with water up to 1:99 (v/v), as seen by the lack of aggregation features in their absorption and emission spectra.

Crystallographic analysis

Scanning electron microscopy (SEM) images of the dried aggregates formed from the *meso*-substituted 1,3,5,7-tetramethyl BODIPY derivatives in 99% (v/v) water/CH_3CN mixtures (Figure 8) suggest that these aggregates are crystalline (300–600 nm × 1700–7500 nm needles for COOMe-**T3**, COO*t*Bu-**T4**, and *i*Pr-**T8**; cubes or plates for CHO-**T5**, CN-**T6**, and Cl-**T7**). X-ray crystallographic studies were carried out to reveal the differing packing modes of these dyes.[17] COOMe-**T3** shows slipped-columns of head-to-head coplanar molecules with an average distance of 3.49 Å between the aromatic planes and a slip angle (θ) of 33° (Figure 9A).[18] This type of packing is replicated for *i*Pr-**T8** (3.65 Å, 36°, Figure 9B) and the previously reported CF_3-**T1** (3.70 Å, 36°).[6] Among these, only COOMe-**T3** and CF_3-**T1** show clear evidence of J-aggregate emission, suggesting that this preferred packing mode is a required but not sufficient condition. In contrast, the X-ray structure of Cl-**T7** shows a herringbone-like (59° tilt) packing of head-to-tail π-stacked dimers that, although close (3.47 Å plane-to-plane distance), present a slip angle representative of H-type packings (65°, Figure 9C), not unlike that found for CH_3-**T2** (65°, 3.55 Å).[6] Both are quenched in the crystal and suspended aggregates.

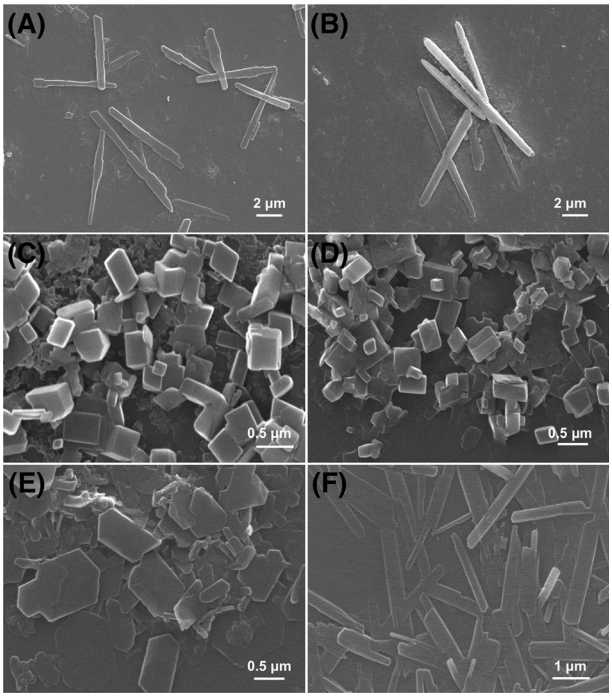

Figure 8. SEM images of COOMe-**T3** (A), COO*t*Bu-**T4** (B), CHO-**T5** (C), CN-**T6** (D), Cl-**T7** (E), and *i*Pr-**T8** (F) aggregates obtained in 99% (v/v) water/CH_3CN mixture. COOMe-**T3**: (454 ± 47) nm/(5039 ± 383) nm, COO*t*Bu-**T4**: (612 ± 61) nm/(7502 ± 1553) nm, CHO-**T5**: (314 ± 20) nm, CN-**T6**: (315 ± 30) nm, Cl-**T7**: (420 ± 84) nm/(834 ± 114) nm, *i*Pr-**T8**: (286 ± 24) nm/(1730 ± 202) nm.

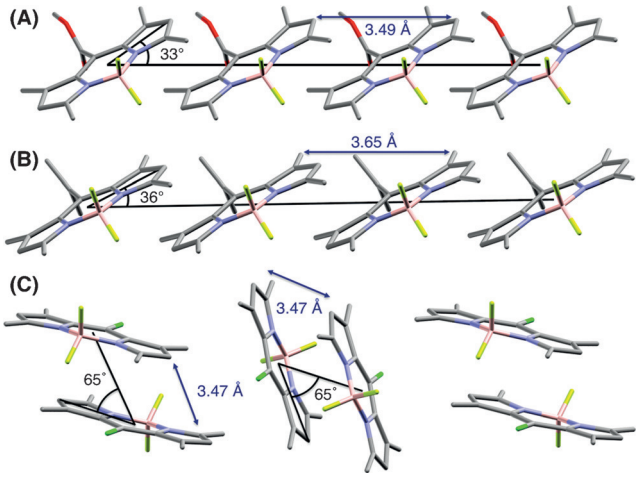

Figure 9. Packing diagrams of COOMe-**T3** (A), *i*Pr-**T8** (B), and Cl-**T7** (C). H atoms are omitted for clarity.

Applications

The emissive J-aggregates formed by COOMe-**T3** can be used as a fully reversible on/off fluorescent probe for organic solvent vapors. As can be seen in Figure 10, a filter paper coated with COOMe-**T3** displays bright orange emission from its J-aggregates upon irradiation with UV light (365 nm). Exposure of this sensing strip at 25 °C to CH_2Cl_2 and $CHCl_3$ vapors for 5 min results in a complete luminescence turn-off. Similar responses are found for 1,2-dichloroethane and acetone vapors after prolonged exposure (30 min). Removal of the solvent by drying the filter paper in air restores the emission, and the sensor strip may be recycled more than 20 times without apparent degradation. The COOMe-**T3**-impregnated filter paper is not responsive to the vapors of hexanes, water, methanol, toluene, and CH_3CN, even upon exposure of up to 10 h. A mechanism in which disruption or solvation of the aggregates occurs upon absorption of the solvent vapors is consistent with this sensing process, which occurs only in the solid state, is non-destructive, and discriminates according to solvating power.

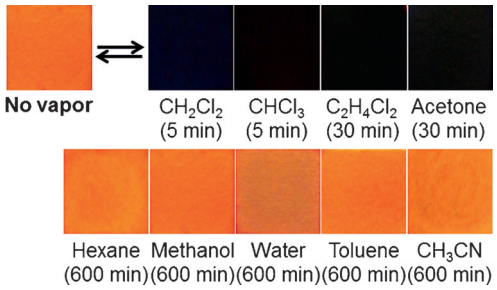

Figure 10. Photographs of the fluorescence of COOMe-**T3** on a filter paper before (left) and after (right) exposure to saturated vapor; under UV light (365 nm) illumination at room temperature. The response time was less than 5 min for CH_2Cl_2 and $CHCl_3$, and approximately 30 min for 1,2-dichloroethane and acetone. The fluorescence of COOMe-**T3** did not change upon exposure to vapors of hexane, methanol, water, toluene, or acetonitrile over the course of 10 h.

Conclusion

This combined experimental and computational study highlights the significant influence of *meso* substituents and their flanking groups at C1 and C7 on the photophysical properties of BODIPY dyes in both solution and the aggregated solid state. In solution, π-conjugated electron-withdrawing substituents at the *meso* position preferentially lower the LUMO level, resulting in redshifted absorption and emission. Flanking methyl substituents can by their steric pressure force the electron-withdrawing group to pivot out of conjugation and the boradiazaindacene core to lose its planarity, resulting in increased nonradiative deactivation rates and lower quantum yields. However, in the aggregated solid state, the combination of an electron-withdrawing *meso* substituent and flanking methyl groups is required for the formation of emissive BODIPY J-aggregates. *Meso*-ester-substituted dyes, such as COOMe-**T3** and COO*t*Bu-**T4**, now join the previously reported CF_3-**T1** as the second class of boradiazaindacene dyes to demonstrably form emissive J-aggregates. Formation of emissive J-aggregates is nevertheless sensitive to minute structural changes, as they are not encountered in the closely related CF_3-**D1**, COOMe-**D3**, COO*t*Bu-**D4** or in other dyes of the **T**-series. Although the potential of these emissive dyes for the selective solid-state sensing of organic solvent vapors was demonstrated, the rich chemistry of the *meso*-carboxyl group[19] now offers new opportunities for fluorescence sensing in the solid state with this family of fluorophores.

Acknowledgements

This research was supported by National Research Foundation of Korea (NRF) grants funded by the Korean government (MSIP) (NRF-2015R1A2A2A01004632 and NRF-2015R1A5A1008958). We thank Dr. Y. Kim of the NanoBio Institute at Ewha Womans University and Dr. H. J. Lee of the Western Seoul Center of the Korea Basic Science Institute for X-ray analysis.

Keywords: aggregation-induced enhanced emission · BODIPY · J-aggregation · solid-state emission · vapor sensing

[1] a) A. Loudet, K. Burgess, *Chem. Rev.* **2007**, *107*, 4891 – 4932; b) G. Ulrich, R. Ziessel, A. Harriman, *Angew. Chem. Int. Ed.* **2008**, *47*, 1184 – 1201; *Angew. Chem.* **2008**, *120*, 1202 – 1219.

[2] a) N. Boens, V. Leen, W. Dehaen, *Chem. Soc. Rev.* **2012**, *41*, 1130 – 1172; b) L. Yuan, W. Lin, K. Zheng, L. He, W. Huang, *Chem. Soc. Rev.* **2013**, *42*, 622 – 661; c) S. C. Dodani, Q. He, C. J. Chang, *J. Am. Chem. Soc.* **2009**, *131*, 18020 – 18021; d) Y. Urano, D. Asanuma, Y. Hama, Y. Koyama, T. Barrett, M. Kamiya, T. Nagano, T. Watanabe, A. Hasegawa, P. L. Choyke, H. Kobayashi, *Nat. Med.* **2009**, *15*, 104 – 109.

[3] a) D. Zhang, Y. Wen, Y. Xiao, G. Yu, Y. Liu, X. Qian, *Chem. Commun.* **2008**, 4777 – 4779; b) T. Ozdemir, S. Atilgan, I. Kutuk, L. T. Yildirim, A. Tulek, M. Bayindir, E. U. Akkaya, *Org. Lett.* **2009**, *11*, 2105 – 2107; c) T. T. Vu, S. Badré, C. Dumas-Verdes, J.-J. Vachon, C. Julien, P. Audebert, E. Y. Senotrusova, E. Y. Schmidt, B. A. Trofimov, R. B. Pansu, G. Clavier, R. Méallet-Renault, *J. Phys. Chem. C* **2009**, *113*, 11844 – 11855; d) G.-L. Fu, H. Pan, Y.-H. Zhao, C.-H. Zhao, *Org. Biomol. Chem.* **2011**, *9*, 8141 – 8146; e) H. Lu, Q. Wang, L. Gai, Z. Li, Y. Deng, X. Xiao, G. Lai, Z. Shen, *Chem. Eur. J.* **2012**, *18*, 7852 – 7861; f) Z. Li, Y. Chen, X. Lv, W.-F. Fu, *New J. Chem.* **2013**, *37*, 3755 – 3761.

[4] a) Y. Hong, J. W. Y. Lam, B. Z. Tang, *Chem. Commun.* **2009**, 4332 – 4353; b) J. Gierschner, S. Y. Park, *J. Mater. Chem. C* **2013**, *1*, 5818 – 5832; c) S. Varughese, *J. Mater. Chem. C* **2014**, *2*, 3499 – 3516.

[5] a) R. Hu, E. Lager, A. Aguilar-Aguilar, J. Liu, J. W. Y. Lam, H. H. Y. Sung, I. D. Williams, Y. Zhong, K. S. Wong, E. Peña-Cabrera, B. Z. Tang, *J. Phys. Chem. C* **2009**, *113*, 15845 – 15853; b) R. Hu, C. F. A. Gómez-Durán, J. W. Y. Lam, J. L. Belmonte-Vázquez, C. Deng, S. Chen, R. Ye, E. Peña-Cabrera, Y. Zhong, K. S. Wong, B. Z. Tang, *Chem. Commun.* **2012**, *48*, 10099 – 10101; c) C. Spies, A.-M. Huynh, V. Huch, G. Jung, *J. Phys. Chem. C* **2013**, *117*, 18163 – 18169; d) C.-L. Liu, Y. Chen, D. P. Shelar, C. Li, G. Cheng, W.-F. Fu, *J. Mater. Chem. C* **2014**, *2*, 5471 – 5478; e) S. Mukherjee, P. Thilagar, *Chem. Eur. J.* **2014**, *20*, 9052 – 9062; f) M. H. Chua, Y. Ni, M. Garai, B. Zheng, K.-W. Huang, Q.-H. Xu, J. Xu, J. Wu, *Chem. Asian J.* **2015**, *10*, 1631 – 1634; g) C. F. Azael Gomez-Duran, R. Hu, G. Feng, T. Li, F. Bu, M. Arseneault, B. Liu, E. Peña-Cabrera, B. Z. Tang, *ACS Appl. Mater. Interfaces* **2015**, *7*, 15168 – 15176.

[6] S. Choi, J. Bouffard, Y. Kim, *Chem. Sci.* **2014**, *5*, 751 – 755.

[7] a) J. B. Birks, *Photophysics of Aromatic Molecules*, Wiley, London, **1970**; b) H. Kuhn, H.-D. Försterling in *Principles of Physical Chemistry, Understanding Molecules, Molecular Assemblies, Supramolecular Machines*, Wiley, New York, **2000**; c) F. Würthner, T. E. Kaiser, C. R. Saha-Möller, *Angew. Chem. Int. Ed.* **2011**, *50*, 3376 – 3410; *Angew. Chem.* **2011**, *123*, 3436 – 3473; d) M. R. Molla, D. Gehrig, L. Roy, V. Kamm, A. Paul, F. Laquai, S. Ghosh, *Chem. Eur. J.* **2014**, *20*, 760 – 771.

[8] E. Palao, A. R. Agarrabeitia, J. Bañuelos-Prieto, T. A. Lopez, I. Lopez-Arbeloa, D. Armesto, M. J. Ortiz, *Org. Lett.* **2013**, *15*, 4454 – 4457.

[9] Y. Ni, L. Zeng, N.-Y. Kang, K.-W. Huang, L. Wang, Z. Zeng, Y.-T. Chang, J. Wu, *Chem. Eur. J.* **2014**, *20*, 2301 – 2310.

[10] K. Krumova, G. Cosa, *J. Am. Chem. Soc.* **2010**, *132*, 17560 – 17569.

[11] M. T. Whited, N. M. Patel, S. T. Roberts, K. Allen, P. I. Djurovich, S. E. Bradforth, M. E. Thompson, *Chem. Commun.* **2012**, *48*, 284 – 286.

[12] J. H. Boyer, A. M. Haag, G. Sathyamoorthi, M.-L. Soong, K. Thangaraj, T. G. Pavlopoulos, *Heteroat. Chem.* **1993**, *4*, 39 – 49.

[13] a) H. Wang, M. G. H. Vicente, F. R. Fronczek, K. M. Smith, *Chem. Eur. J.* **2014**, *20*, 5064 – 5074; b) V. Leen, P. Yuan, L. Wang, N. Boens, W. Dehaen, *Org. Lett.* **2012**, *14*, 6150 – 6153.

[14] Owing to the rapid formation of hydrates (R–$CH(OH)_2$) in aqueous solution, the photophysical behavior of CHO-**D5** in the CH_3CN/H_2O solvent system could not be investigated.

[15] a) C. Hansch, A. Leo, R. W. Taft, *Chem. Rev.* **1991**, *91*, 165 – 195; b) I. K. Petrushenko, K. B. Petrushenko, *Spectrochim. Acta Part A* **2015**, *138*, 623 – 627.

[16] a) J. Bañuelos Prieto, F. L. Arbeloa, V. M. Martínez, T. A. López, I. L. Arbeloa, *J. Phys. Chem. A* **2004**, *108*, 5503 – 5508; b) J. Jayabharathi, V. Thanikachalam, R. Sathishkumar, *Spectrochim. Acta Part A* **2012**, *97*, 582 – 588.

[17] CCDC 1416493 (COOMe-**T3**), 1416492 (Cl-**T7**), and 1416494 (*i*Pr-**T8**) contain the supplementary crystallographic data for this paper. These data are provided free of charge by the Cambridge Crystallographic Data Centre.

[18] All attempts at the crystallization of COOMe-**T3** led to very thin plates that resulted in a low quality X-ray structure.

[19] S. Kim, H. Kim, Y. Choi, Y. Kim, *Chem. Eur. J.* **2015**, *21*, 9645 – 9649.

Received: August 3, 2015
Published online on October 14, 2015